EVALUATION OF CABIN DISPLACEMENT VENTILATION UNDER FLIGHT CONDITIONS

J. Bosbach*[1], A. Heider*, T. Dehne*, M. Markwart, I. Gores**, P. Bendfeldt****
***German Aerospace Center (DLR), Institute of Aerodynamics and Flow Technology,**
Bunsenstr. 10, 37073 Göttingen, Germany, **Airbus Operations GmbH,
Environmental Control Systems, Kreetslag 10, 21129 Hamburg, Germany
[1]Johannes.Bosbach@dlr.de

Keywords: *indoor air flow, displacement ventilation, environmental control, flight test*

Abstract

For the first time cabin displacement ventilation (CDV) has been tested under flight conditions in a passenger aircraft cabin. We were able to validate the expected advantages of CDV in a reconfigured part of an A320 aircraft. A cabin flight test and a CDV installation, suitable for static as well as dynamic ground and flight tests were developed. Pure CDV provides low air velocities and turbulence levels, a high heat removal efficiency and a very good dynamic performance. Providing 30% of the total volume flow rate through the lateral outlets in a hybrid system allows for still comfortable flow velocities and good heat removal efficiency, yet improves the temperature stratifications and the cooling and heating rates at the cabin surfaces. Both systems provide a very homogeneous temperature distribution among the different seat positions.

1 Introduction

Conventional ventilation systems for passenger aircraft are based on the principle of mixing ventilation (MV), where fresh air is blown into the cabin via jets of rather high momentum [1], see Fig. 1a). These jets lead to a controlled mixing of fresh and used air by entrainment. After circulation in the cabin, the air leaves below the dado-panels at floor level. In view of the fact that since a few years there is a general trend of increasing heat loads to be observed in modern passenger aircraft cabins, a severe drawback of MV is, that it is prone to draught at high heat load densities. Further potentially critical issues in MV systems are acoustical noise, distribution of pollutants, exsiccation of mucosa, limited flexibility regarding cabin (re)configurations and a relatively high amount of short circuit flows. Displacement ventilation (DV) is expected to be far less susceptible to many of these issues and therefore application of DV to air conditioning of aircraft cabins (CDV – cabin displacement ventilation) has been investigated recently [2][3][4][5]. CDV is based upon the supply of fresh air into the cabin with low velocity, often at floor level, and extraction close to the ceiling, see Fig. 1a). The fresh air is heated by thermal loads, like e.g. passengers, and rises in their vicinity due to buoyancy. Consequently, every passenger generates its own fresh air bubble. This leads to much lower fluid velocities and a far higher heat-removal efficiency of CDV as compared to MV. However, all of the studies reported so far were either numerical or conducted on a laboratory scale. Validation of the advantages under real conditions, which is the scope of our study, has still been lacking.

2 Ventilation of Aircraft Cabins

Since a few years a growing interest regarding alternative ventilation concepts for aircraft can be observed in the literature, which has been mainly driven by the issues thermal passenger comfort and as well as contaminant distribution and removal [2-7].

In order to overcome the deficiencies of MV, mainly two approaches have been investi-

gated, namely CDV and personalized air distribution systems. Schmid et al. [3] and Müller et al. [2] studied and compared MV and CDV in a A320 mock-up cabin section. In addition to pure MV and CDV also a hybrid CDV system with support of the lateral air inlets was studied (see Fig. 1c).

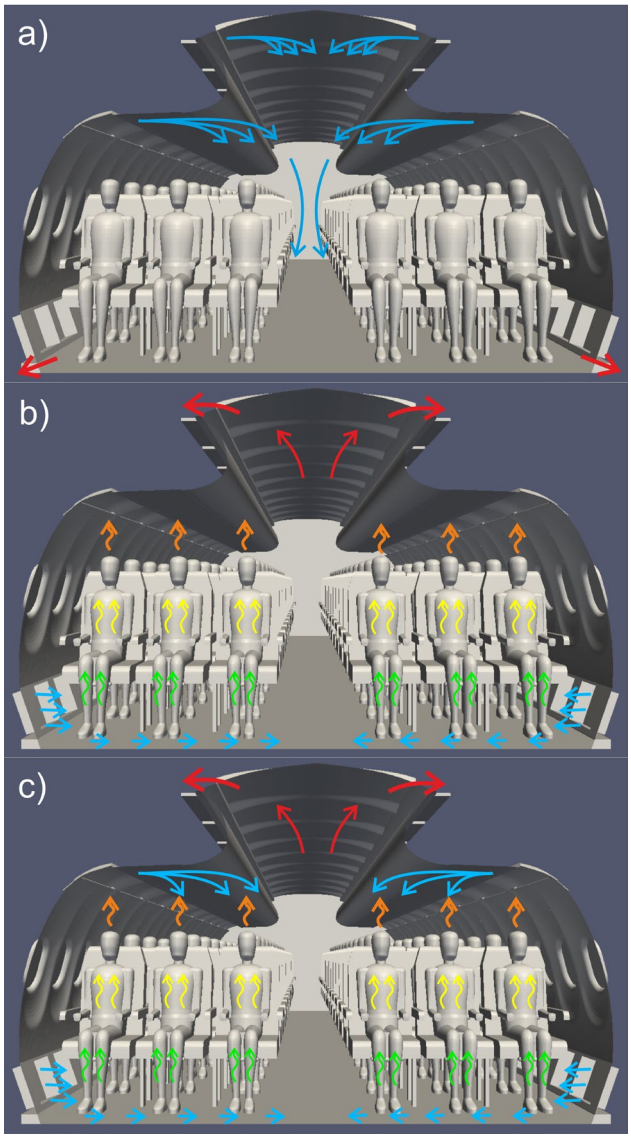

Fig. 1. Illustration of different ventilation principles. a) mixing ventilation (MV), b) displacement ventilation (CDV), c) combination of CDV and MV (HV – "hybrid ventilation"). For further explanations, see text.

Schmid et al. see advantages and drawbacks for both systems. While MV bears a higher draft risk, CDV tends to "hot heads". However, as long as the temperature difference between feet and heads is kept in a comfortable range, Müller et al. see CDV in advance. Zhang et al. [5] used CFD to compare different ventilation concepts in a Boeing 767 aircraft cabin section, namely a MV, an aisle under-floor CDV and a personalized air distribution system with respect to temperature, velocity and CO_2 distributions. They conclude, that the personalized air distribution system, providing outside air into the passengers breathing zone, created the best cabin environment. MV, at the other end of the scale, generated the most uniform air temperature, but the highest air velocities and CO_2 concentrations. Comparison, however, of MV and CDV in the same configuration let Yin et al. [4] recommend CDV for possible use in future airplanes according to its good performance: CDV was found to lessen the CO_2 concentrations by 30% and improve the relative humidity from 12% to 22% without causing condensation risks.

While some studies already consider moving obstacles [7] or transient effects [8], none of the studies reported so far addressed the issues efficiency and performance, which are important factors to complete the image of the different ventilation concepts.

3 Aircraft

3.1 General Description

With the intention to validate the expected advantages of CDV under real conditions, the "Advanced Technology Research Aircraft" (ATRA) of the German Aerospace Center (DLR) was chosen as test platform. ATRA is an Airbus A320-232 (MSN659) and the largest test bed of the DLR fleet.

3.2 Cabin Layout

For evaluation of CDV at ground and flight conditions, approximately one half of the ATRA cabin was refurbished with a CDV system, see Fig. 2. The measurement section extended from C45 to C62. It was separated by foam walls of 0.5 m thickness on each side from the rest of the cabin in order to ensure thermal insulation and to prevent air exchange. The remaining part of the cabin was used to install operator and measurement racks of the flight test installation (FTI).

3.3 Integration of Cabin Displacement Ventilation

The CDV system provides fresh air at low momentum through specially developed CDV outlets. The new outlets replaced the former dado-panels after shortening of the side panels, see Fig. 1b). In addition, a fraction of fresh air could be supplied through the preexisting lateral MV outlets, while exhaustion of air was provided mainly through the preexisting ceiling outlets, see Fig. 1b), c). The CDV outlets were not only designed to provide a homogeneous distribution of the volume flow among their active surface of 0.11 m² (3.68 m² for the whole measurement section), but also ensured rapid decompression in case of a sudden pressure drop in the cabin. For extraction of the air from the cabin the former ceiling outlet tubing system was simply left open in order to allow the used air to leave the cabin through the pre-existing openings and gaps.

Measurement, calibration and control of the volume flow rates in the different ducts was accomplished by a measurement system capable to access static pressures at 17 positions and fluid temperatures at 5 positions in the duct system in combination with four manually adjustable iris diaphragms.

4 Flight Test Installation

4.1 General Description

A cabin FTI comprising 63 passenger thermal dummies, 14 sensor racks, an automatically rotatable infrared camera and a dual color laser light sheet for flow visualization was developed and installed in order to capture the relevant flow phenomena and to simulate the heat impact of the real passengers (Fig. 3). In total more than 200 sensors were installed in the test section.

4.2 Thermal Passenger Dummies

A key component of our FTI constitute the thermal passenger dummies (TPDs), which ensure realistic heat loads and obstructions. The TPDs have a volume of 0.05 m^3, a surface of 1.5 m^2 and are operated under constant heat flux conditions by two specially designed power supplies, which are mounted in the FWD zone. The main advantage of the employed TPDs is the very homogeneous heat flux density, which is slightly increased on purpose in the head region. A homogeneous distribution of the heat load over the TPD surface is a necessity in order to accomplish realistic surface temperatures and thus buoyancy forces. For the results described in the following, the heat flux of the TPDs was set to an average value of 75W/TPD. The TPDs were arranged in 11 seat rows in the measurement section with a seat pitch of 31” (Fig. 2). The supply cables of the TPDs were routed at floor level below the seats. They released another 400 W of thermal energy into the measurement section.

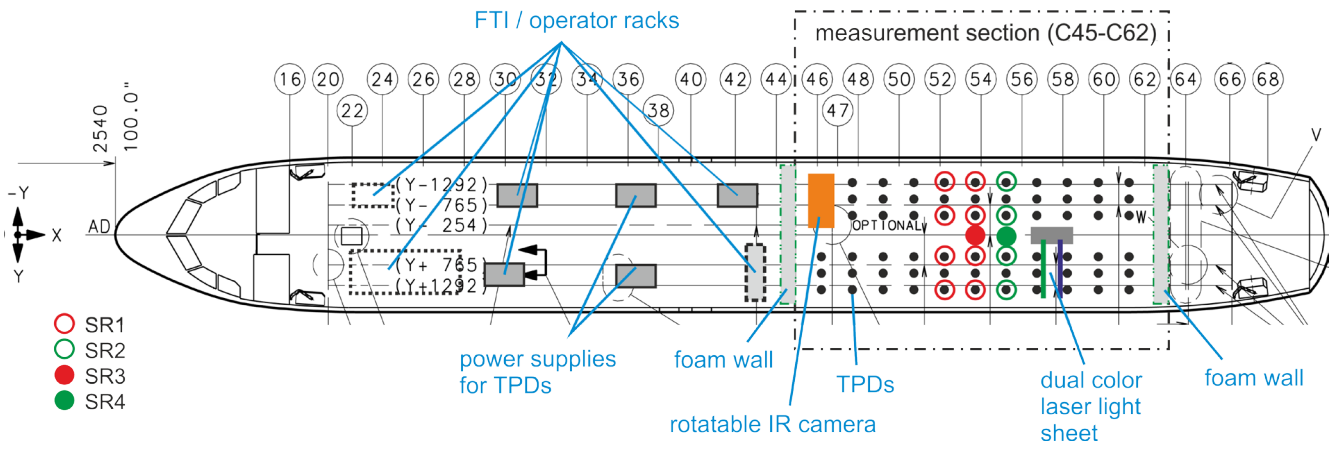

Fig. 2. Cabin layout and main components of the cabin flight test installation.

Fig. 3. Photographs of the flight-test installation in the measurement section. a) Automatically rotateable infrared camera set-up for acquisition of surface temperature panoramas during the flight, b) thermal passenger dummies, sensor racks and surface temperature sensors, c) thermal passenger dummies and SR1 sensor rack.

4.3 Sensor Racks

Fluid temperatures and velocities were measured near the TPDs in three rows as well as in the aisle region, with the aim to judge the achievable thermal comfort for passengers and crew from objective data, see Fig. 3b) and c). The sensors were mounted on four different types of sensor-racks, which we refer to as SR1, SR2, SR3 and SR4, see Fig. 2. While SR1 and SR2 were positioned near the TPDs at the aisle and window seats, SR3 and SR4 placed their sensors centrally in the aisle between the shoulders of the adjacent TPDs. Two consecutive seat rows were equipped with SR1s, which comprised combined omnidirectional velocity and temperature probes at three levels (ankle, knee and head) and a reference temperature sensor (RTD – resistance temperature detector) at chest level. The following seat row was equipped with SR2s, which comprised RTDs at 10 height levels. All SR1 and SR2 racks were equipped with globe temperature sensors with a diameter of 40 mm at chest level. The sensors in the upper body half were mounted at the body centerline, while the sensors in the lower body half, starting at knee level, were installed centrally in front of the aisle and wall sided leg of the aisle and window seats, respectively. Only the sensors at ankle and ear (SR2) level were fixed aside the outside ankle (ear for SR2) of the aisle and wall-sided leg (ear for SR2) of the aisle and window seats, respectively. Using the sensor placement described above, ensures, to our appraisement, access to the most comfort-critical positions as compared to a simple central alignment of the sensors with respect to the TPDs.

The heat load of the passengers, or as in our experiment, the TPDs, is one driving force of the cabin air flow and thus has a significant impact on the temperature and velocity distribution in their proximity. Hence, the probes were installed close to the TPDs at a distance of 5 cm +/- 0.5 cm apart from the surface, i.e. outside of the thermal and velocity boundary layers, yet close enough to capture the climate in the very surrounding of the TPDs.

The sensor racks SR3 and SR4 were used to instrument the aisle region with the objective to capture the time dependent temperature stratification as well as the velocity distribution here. SR3 was equipped with combined omnidirectional velocity and temperature sensors at 7 levels, while SR4 comprised RTDs at 12 levels. Since no TPDs were employed in the aisle the sensor racks were much simpler and just consisted of a vertical arrangement of the sensors.

In order to account for the varying cabin pressure, the signal of the omnidirectional velocity probes has been pressure corrected appropriately prior to further evaluation.

4.4 Further Instrumentation

Capturing the thermal boundary conditions during the flights was ensured by 24 RTDs glued with painted aluminum tape on the interior floor, hat-rack, side-panel, windows and

ceiling panel surfaces. 20 additional RTDs were installed in the CDV, lateral and ceiling air outlets. The temperatures of the 12 TPDs, which had sensor racks installed in front, were measured with RTDs fixed at the back of their heads.

Although no humidity sources were on board (except for the flight test personnel), the air humidity was measured with a dew point transmitter, which was mounted to one of the sensor racks in the aisle just below the ceiling. A capacitance absolute pressure sensor was used to record the cabin pressure during the whole flight. All other pressures, see sec. 3.3, were measured relatively to the cabin pressure. The respective measurement hoses were combined in a settling chamber, which was mounted together with the pressure sensors on vibrational dampers in a common housing.

Beyond the sensors described so far, which provide measures from the inside of the aircraft cabin, the basic FTI of ATRA was configured to record all flight test data of relevance for our experiment, as outside temperature, outside pressure, altitude, flight attitude, flight velocity, GPS coordinates and many more.

4.5 Infrared Camera

Complementary to the surface sensors, a programmable, step motor driven, automatically rotatable infrared camera set-up was installed in the front of the measurement section, see Fig. 3a) and Fig. 2. The appliance is able to rotate the mounted IR camera around two axes and thus allowed to take a panorama image of the whole cabin interior every minute.

4.6 Flow Visualization

Visualization of the cabin air flow was achieved using two portable fog-guns and a portable HD camcorder. As a light source a dual color laser light sheet set up was employed. It allows for simultaneous visualization in two different measurement planes and consists of two continuous wave diode pumped solid state lasers in combination with two light sheet optics. The set-up was mounted in the aisle and fixed to the seat rails. Both light sheets had a thickness between one and two mm and were adjusted to be perpendicular to the aircraft axis. The green light sheet with a wavelength of 532 nm was placed just 45 mm behind the seat of the 8th seat row, the blue light sheet with a wavelength of 445 nm was positioned 70mm in front of the torso of the TPDs in the 9th seat row, see Fig. 2.

5 Investigated Climate Scenarios

Different ground and flight tests were conducted under both, steady and unsteady conditions. In the following two distinct climate scenarios will be discussed: pure CDV (“CDV”) and a hybrid case (“HV”). At CDV 100% of the air flow rate was provided through the CDV outlets (compare Fig. 1b). At HV 70% of the air flow rate was provided by the CDV outlets while the original A320 lateral outlets provided 30% (compare Fig. 1c).

	CDV ground	CDV flight	HV ground	HV flight
q_V [l/s]	743(7)	721	732	717(2)
P_{TPD} [kW]	4.73	4.73	4.73	4.73
P_{Cable} [kW]	0.40	0.40	0.40	0.40
P_{light} [kW]	2.00	2.00	2.00	2.00
p [hPa]	1022	768	1024	768(5)
Ma	0	0.78	0	0.78
ALT [ft]	16	37154.. 37251	16	37267.. 38339

Tab. 1. Measurement conditions for the investigated steady climate scenarios. q_V denotes the volume flow rate, P_{TPD} the total heating power of all TPDs, P_{Cable} the total heating power of the TPD supply cables, P_{light} the total heating power of the light bands, p the cabin pressure, Ma the Mach number and ALT the altitude. The numbers in brackets give the standard deviation if the variations exceed the last digit.

The measurement conditions for the steady scenarios are summarized in Tab. 1. However, the values for the dynamic scenarios, which are discussed in sec. 6.5, are almost identical. During the tests the window shutters in the measurement section were closed in order to prevent heating of the sensors by solar radiation. The cabin illumination was switched on except during the laser light sheet flow visualizations. Pri-

or to the ground tests the TPDs and the ventilation system were running for at least 85 minutes before counting the data in order to achieve static climate conditions. For the same reason we waited at least another 87 minutes after reaching flight level before considering the test data for evaluation of the time-averaged quantities. The duration of the whole test flight amounted more than 5 h at flight level and more than 6:30h including the ground tests for each scenario. All sensor signals have been averaged over a period of 600 s for all discussed scenarios.

6 Experimental Results

6.1 Flow Visualizations

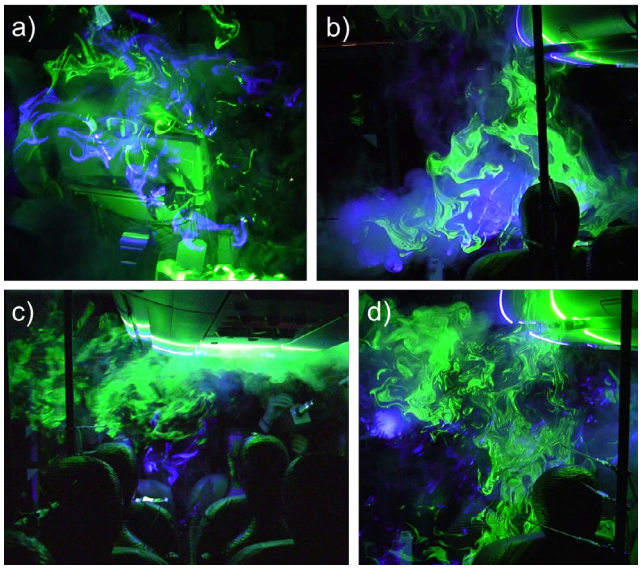

Fig. 4. Visualization of the cabin flow using the two-color laser light sheet. a) Flow behind a seat, CDV, b) flow at head level, CDV, c) lateral air jet, HV and d) flow at head level, HV.

Visualizations of the cabin air flow under flight conditions are depicted in Fig. 4. For pure CDV the structures in Fig. 4a) and b) were created during emission by the fog gun. The fluid itself is moving very slowly in most parts of the cabin. Exceptions are the very vicinity of the TPDs, i.e. the boundary layers, as well as the region between the overhead bins. Consequently the observed structures are very stable except for the regions close to the TPD heads, where a locally increased upward motion of the fluid can be detected in the selected light sheet planes. Further visualizations between the overhead bins, not shown here for the sake of brevity, clearly reveal, that the air rises up to the ceiling and leaves the cabin in the crown area, proving functionality of the concept of passive air extraction.

Qualitatively very different are the visualizations for HV (Fig. 4c and d). The lateral air jets induce a higher level of turbulence, which is reflected by a larger amount of small scales in the fog distribution. Since the lateral air jet just carries 30% of the volume flow rate it interacts quite strongly with the rising hot air above the TPD heads. This leads to a three dimensional broadening and breakup of the wall jet and thus to large-scale circulations oriented horizontally between the seats, which, in addition to the increased turbulence level, might precipitate the exchange of particles/pathogens or CO_2 between seats and rows. Nevertheless, it can still be observed, that the air ascends preferably near the TPDs, which ensures a high cooling efficiency.

6.2 Infrared Thermography

Panorama views of the surface temperature distribution during steady flight conditions are shown in Fig. 5. We would like to stress here, that the elevated head temperatures of the TPDs are mainly caused by the increased local heat flux density in this region. A very homogeneous temperature distribution among the different seat positions can be observed. A systematic difference can be detected between the window seats at both sides: while the window temperatures on the right hand side (in flight direction) are of the order of the inflow temperature, elevated window temperatures are found on the left hand side, which are caused by solar radiation. Consequently, even though the window shutters were closed, this has an impact on the torso temperature of e.g. the rightmost TPD. Another region of rather low surface temperatures is the floor, which is not only caused by the fact that the fresh air is injected at floor level, but also because the air volume in the cargo compartment serves as a remarkable heat reservoir. By comparing HV with CDV one can discover that the mean torso temperature of the TPDs is higher for hybrid ventilation as compared to CDV,

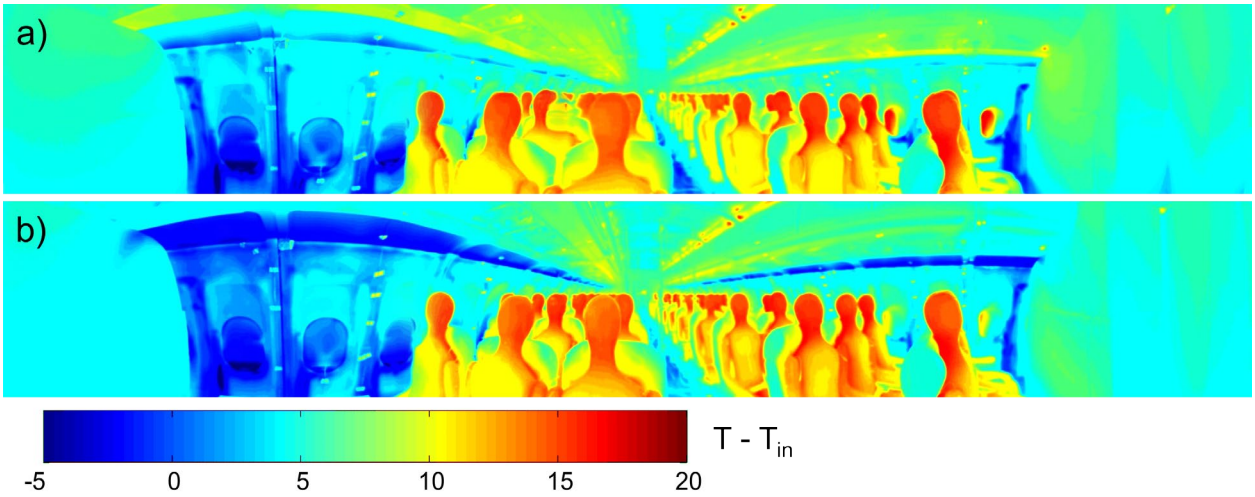

Fig. 5. 360° Panorama views of the surface temperatures, measured using the automatically rotatable infrared camera set-up. Depicted is the difference between surface temperature and mean inflow temperature. a) "CDV flight", b) "HV flight".

indicating a higher local air temperature. The other significant difference is that for HV the lateral air outlets, hat racks and sidewalls are cooler as compared to CDV.

6.3 Fluid Temperatures

Representative for the plethora of temperature stratifications measured during the different flight phases in the cabin, Fig. 6 depicts the temperature profiles for the stationary ground and flight tests for CDV and HV in the aisle (SR4). The temperatures are given relative to T_{Cabin}, which is the average of the measured temperatures at ankle, knee, head and chest level of all SR1s and SR2s.

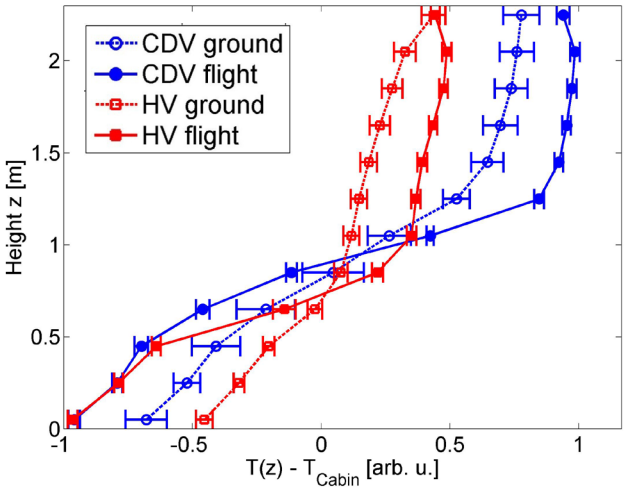

Fig. 6. Mean temperature stratifications in the aisle region, measured with SR4. The temperatures are given as differences to T_{Cabin} in arbitrary units. The error bars indicate the temporal standard deviations of the data.

First, we would like to discuss the flight scenarios. By looking at the data for "CDV flight" two distinct regions can be distinguished: while a rather steep stratification is observed for $z < 1.3$ m, i.e. in the region where the TPDs are located, the change with height is much weaker for $z > 1.3$ m. Switching from CDV to HV, however, allows to significantly reduce the total temperature stratification. A closer look to the data reveals that this is due to an absolute increase of the temperatures in the lower cabin part caused by the reduced volume flow rate through the CDV outlets and mixing of the air induced by the lateral wall jets. Comparison of the flight cases with the ground cases reveals that with the same volume flow rate, i.e. a mass flow rate increased by 33 %, the temperature stratifications are much weaker.

6.4 Flow Velocities

The flow velocities near the TPDs, as measured with the SR2s, are summarized in Fig. 7 for the flight cases. As expected, the velocities are very small for CDV, and the average values do not exceed 0.15 m/s. The highest velocities are observed at knee level at the window seats, i.e. close to the CDV outlets, but even if fluctuations (standard deviations) are taken into account, the values in this region stay well below 0.21 m/s. At the other measurement positions, the velocities are even smaller.

Upon switching to HV, the velocity distribution changes qualitatively: Due to the reduced

momentum of the CDV flow the elevated values at knee level of the window positions is significantly reduced, however the velocities in the head region of the aisle positions in turn increase and exceed the values found for CDV before. Nevertheless even under consideration of the standard deviations the values stay below 0.26 m/s. The results for the ground tests look very similar and are not shown here for the sake of brevity.

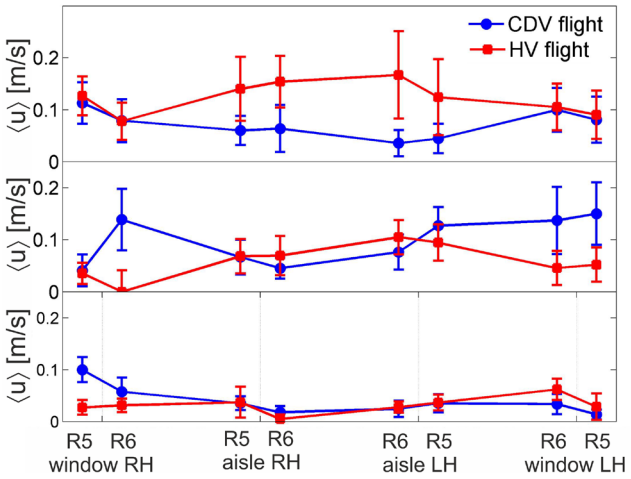

Fig. 7. Mean flow velocities near the thermal passenger models, measured with the SR2s. The error bars indicate the temporal standard deviations at the respective measurement position. a) head (z = 1.25 m), b) knee (z = 0.55 m) and c) ankle (z = 0.07 m) level.

6.5 Dynamic Measurements

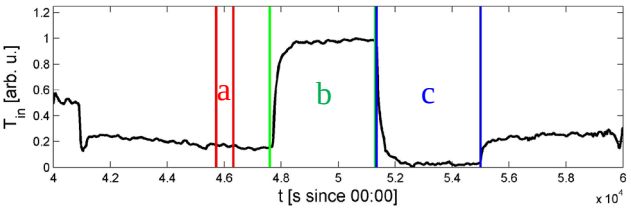

Fig. 8. Climate phases during "CDV flight" visualized by the mean inflow temperature as a function of time: a) stationary, b) pull-up, c) pull-down.

So far, only the stationary behavior of the two investigated ventilation systems has been discussed. Besides the stationary performance, however, the dynamic response of the environmental control system is important for approval as well. In order to characterize the performance of the two ventilation systems the inflow temperature has been elevated ("pull-up") and lowered ("pull-down") in steps ΔT_p of approximately 10 K subsequent to the stationary measurements, see Fig. 8. The changed inflow temperatures were kept for at least 45 min. Meanwhile the cabin FTI recorded the transient temperature and velocity profiles. Results for the mean cabin temperature, mean floor, mean hat rack and average surface temperatures are depicted in Fig. 9 for CDV. The given values are the differences to the temperature prior to the "pull-up" or "pull-down", normalized to the respective temperature jump ΔT_p.

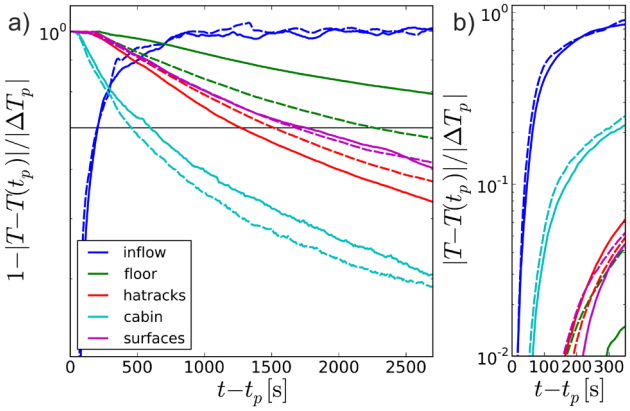

Fig. 9. Normalized temperature differences as a function of time for the "pull-up" (solid lines) and "pull-down" (dashed lines) scenario for "CDV flight" in different scalings. "inflow", "floor" and "hatracks" denote the mean inflow, floor and hatrack temperatures as measured with the local RTDs, respectively. "cabin" denotes the average of all temperature sensors near the TPDs at ankle, knee, chest and head level in the 8th seat row (SR2) and serves as a measure of the mean cabin temperature. "surfaces" denotes the average surface temperature, calculated from the mean of the temperatures measured at ceiling, sidepanels, hat racks and floor with the local RTDs.

Fig. 9 reveals that the cabin temperature reacts quite fast to the changed inflow temperature. The pull-down is significantly faster than the pull-up, which we ascribe to the fact, that during pull-down the fresh air is attracted by the dummies more efficiently due to buoyancy. The surface temperatures, especially in the lower cabin part, react much more slowly. During pull-down the cold air accumulates at the floor, resulting in a higher cooling rate as compared to the pull-up scenario. Fig. 9a) reveals, that the time responses of the temperatures do not follow simple exponential decays. We ascribe this behavior to the interplay of heat transition and subsequent thermal diffusion inside the cabin materials and foams during pull-up and pull-down, respectively. Since the interior materials contain

a high fraction of air, the distribution of heat inside these materials is very slow and thus limits its heat transition between fluid and surfaces. Consequently, even after 2500 s none of the investigated temperatures in Fig. 9 reaches the applied temperature jump.

$t_{0.01}$ [s]	pull-up	pull-down
cabin (CDV)	50	40
cabin (hybrid)	70	50
surface (CDV)	200	140
surface (hybrid)	30	160

Tab. 2. Times required for a temperature change of 1% of the applied inflow temperature jump ΔT_p .

$t_{0.3}$ [s]	pull-up	pull-down
cabin (CDV)	510	390
cabin (hybrid)	630	590
surface (CDV)	1670	1620
surface (hybrid)	980	1110

Tab. 3. Times required for a temperature change of 30% of the applied inflow temperature jump ΔT_p .

Since the pull-up / -down performance cannot be characterized by a simple time constant, we calculated two different quantities. As a means to quantify how long it takes for a specific temperature to react to the changed inflow temperature we calculated $t_{0.01}$, which is the time required for a 1% temperature change of ΔT_p (see Tab. 2) counted from the time that the inflow temperature changed by more than 1% of ΔT_p. In order to quantify the time required for an effective temperature change, we evaluated $t_{0.3,}$ which describes the time required to reach 30% of ΔT_p counted from the time that the inflow temperature changed more than 30% of ΔT_p (see Tab. 3). All times in Tab. 2 and Tab. 3 were rounded to 10 s.

Comparison of $t_{0.3}$ for CDV and HV reveals that the cabin temperature change is always faster for CDV as compared to HV. With both systems, however, a temperature change of 3 K was possible within less than 11 minutes. A different situation is found for the surface temperatures, which can be changed between 30 and 40% faster with HV as compared to CDV due to the impact of the additional lateral wall jet.

A closer look to $t_{0.01}$ shows that the cabin temperature reacts within a time of less than 70 s in all cases, while the surfaces may require more than 3 minutes, depending on the ventilation system and scenario. One reason for this finding is, that prior to the surface temperature reaction the air has to be changed in order to allow for a temperature difference and thus heat flow between fluid and surfaces. Consequently, the surface temperatures react mostly after a few nominal air changes, which is reflected in a delayed temperature response, see Fig. 9b).

6.6 Heat Removal Efficiency

Besides thermal comfort and dynamic performance, an important aspect of alternative ventilation concepts is the heat removal efficiency. The heat removal efficiency at a fixed volume flow rate is proportional to the amount of thermal energy, which the air has absorbed in the cabin, i.e. the temperature difference between exhausted air and incoming air. On the other hand the cooling efficiency is understood to be poor if the temperature difference between cabin and incoming air is high. Accordingly a "heat removal efficiency" (*HRE*) can be defined as

$$HRE = 0.5 \frac{(T_{exit} - T_{in})}{(T_{Cabin} - T_{in})} . \qquad (1)$$

The *HRE* of a perfect MV system would be 0.5, while the *HRE* of real MV systems are expected to be of the order of 0.4. During static flight conditions we observed *HRE* = 0.98 for CDV and *HRE* = 0.66 for HV. Correspondingly cooling of heat loads is more efficient employing CDV by a factor of 2 or more as compared to MV. Supply of 30% of the fresh air through the lateral inlets results in higher short circuit flows, which is reflected in a reduction of the HRE by about 30% as compared to CDV. However, the HRE of HV is still significantly higher as compared to MV.

7 Conclusions

For the first time cabin displacement ventilation has been tested under flight conditions in a passenger aircraft cabin. Two variations, i.e.

pure cabin displacement ventilation (CDV) and a hybrid ventilation system (HV) were studied. While at CDV the fresh air rises only in the vicinity of the heat loads and leaves the cabin through the open ceiling outlets, a higher degree of mixing and thus turbulence was observed at HV in the flow visualizations. The different turbulence structure implicates several characteristic differences between the two ventilation concepts, which were proven experimentally. While the surface temperature distributions are homogeneous among the different seat positions, a higher TPD chest temperature and lower relative wall temperatures already distinguishes HV. Measurements of temperature stratifications in the fluid reveal that at HV the total vertical temperature stratification is lower by one third as compared to CDV. Another way to achieve this is to increase the mass flow rate, as indicated by the ground test data. The fluid velocities near the TPDs are overall very low for both systems. HV tends to higher velocities at the aisle seats, which, however, are far too low to become comfort-critical. The systems further differentiate when dynamic scenarios are studied. Both, HV and CDV are able to reduce or increase the cabin air temperature by 3 K within less than 11 minutes at flight conditions. However, CDV performs better for the cabin air temperature, while HV is faster when it comes to cooling of the surfaces. For all ventilation systems thermal diffusion inside the cabin materials limits the long-term dynamics. CDV distinguishes itself by the fact of the largest observed heat removal efficiency, which amounted to almost one at flight conditions. HV still has a much smaller but still high efficiency of 0.66. Flight tests to study the state of the art mixing ventilation under flight conditions are planned and will provide a reliable baseline for scoring the different concepts.

Acknowledgements

Supported by:

Federal Ministry of Economics and Technology

on the basis of a decision by the German Bundestag

This project was supported by the German Federal Ministry of Economics and Technology under the grant numbers 20K0806D, 20K0806A and 20K0702A on the basis of a decision of the German Bundestag. The responsibility of the content is the authors.

We thank all colleagues at Airbus Operations and the German Aerospace Center, who contributed to the successful preparation and performance of the ground and flight tests.

References

[1] Kühn M, Bosbach J, Wagner C. Experimental parametric study of forced and mixed convection in a passenger aircraft cabin mock-up, *Building and Environment*, Vol. 44, No. 5, pp 961-970, 2009

[2] Müller D, Schmidt M, Müller B. Application of a Displacement Ventilation System for Air Distribution in Aircraft Cabins, *AST 2011*, March 31 – April 1, Hamburg, Germany, 2011

[3] Schmid M, Müller D, Gores I, Markwart M. Numerical Study of Different Air Distribution Systems for Aircraft Cabins, *11th International Conference on Indoor Air Quality and Climate*, 17th August to 22nd August, Copenhagen, Denmark, 2008

[4] Yin S, Zhang T. A New Under-Aisle Displacement Air Distribution System for Wide-Body Aircraft Cabins, *Eleventh International IBPSA Conference*, Glasgow, Scotland, pp 1030-1036, 2009

[5] Zhang T, Chen Q. Novel air distribution systems for commercial aircraft cabins, *Building and Environment*, Vol. 42, No. 4, pp 1675-1684, 2007

[6] Zhang Z, Chen X, Mazumdar S, Zhant T, Chen Q. Experimental and numerical investigation of airflow and contaminant transport in an airliner cabin mockup, *Building and Environment*, Vol. 44, pp 85-94, 2009

[7] Mazumdar S, Chen Q. Impact of moving bodies on airflow and contaminant transport inside aircraft cabins, *Roomvent 2007*, Helsinki, Finland, 2007

[8] Bianco V, Manca O, Nardini S, Roma M. Numerical investigation of transient thermal and fluidynamic fields in an executive aircraft cabin, *Applied Thermal Engineering*, Vol. 29, pp 3418-3425, 2009

Copyright Statement